Mon. Not. R. Astron. Soc. **312**, 371–379 (2000)

Galaxy formation and evolution – II. Energy balance, star formation and feedback

Fulvio Buonomo,[1★] Giovanni Carraro,[1★] Cesare Chiosi[1★] and Cesario Lia[2★]
[1]*Dipartimento di Astronomia, Università di Padova, Vicolo dell'Osservatorio 5, I-35022 Padova, Italy*
[2]*SISSA-ISAS, via Beirut 2-4, I-34013 Trieste, Italy*

Accepted 1999 September 23. Received 1999 September 14; in original form 1998 January 21

ABSTRACT

In this paper we present a critical discussion of the algorithms commonly used in *N*-body simulations of galaxy formation to deal with the energy equation governing heating and cooling, to model star formation and the star formation rate, and to account for the energy feedback from stars. First, we propose our technique for solving the energy equation in the presence of heating and cooling, which includes some differences with respect to the standard semi-implicit techniques. Secondly, we examine the current criteria for the onset of the star formation activity. We suggest a new approach, in which star formation is allowed to depend on the total mass density – baryonic (gas and stars) and dark matter – of the system and on the metal-dependent cooling efficiency. Thirdly, we check and discuss the separate effects of energy (and mass) feedback from several sources – namely supernovae, stellar winds from massive stars and ultraviolet flux from the same objects. All the simulations are performed in the framework of the formation and evolution of a disc galaxy. We show that the inclusion of these physical phenomena has a significant impact on the evolution of the galaxy models.

Key words: hydrodynamics – methods: numerical – stars: formation – galaxies: evolution – galaxies: formation.

1 INTRODUCTION

Numerical hydrodynamics and *N*-body simulations are nowadays the fundamental tools to investigate galaxy formation and evolution. The current status of numerical and semi-analytical modelling of various galaxy properties has recently been summarized by Frenk et al. (1997).

One poorly understood process is the formation of stars. Since the pioneering study by Katz (1992), the onset of star formation (SF) is usually empirically parametrized (see also Gerritsen 1997). The key idea is that an element of fluid must satisfy some conditions in order to be eligible for SF and turn part of its gas content into stars at a suitable star formation rate (SFR), which is customarily reminiscent of the Schmidt (1959) law. The reader is referred to the exhaustive discussion of this topic by Mihos & Hernquist (1994) for more details.

The basic criteria to select the fluid elements prone to SF are (i) the gas particle must be in a convergent flow, and (ii) the gas particle must be Jeans unstable. The conditions are met if the velocity divergence is negative and if the sound crossing time-scale is shorter than the dynamical time-scale.

★ E-mail: buonomo@pd.astro.it (FB); carraro@pd.astro.it (GC); chiosi@pd.astro.it (CC); liac@sissa.it (CL)

Schmidt-like laws imply that SFR $\propto \rho^n$, where the power n ranges between 1 and 2. Conservation arguments suggest that the most probable value of n is $\frac{3}{2}$ (see Katz 1992). The Schmidt law written for the volume density is

$$\frac{\mathrm{d}\rho_\star}{\mathrm{d}t} = -\frac{\mathrm{d}\rho_\mathrm{g}}{\mathrm{d}t} = \frac{c_\star \rho_\mathrm{g}}{t_\mathrm{g}} \tag{1}$$

where $c_\star$ is the so-called dimensionless efficiency of star formation, and t_g is the characteristic time for the gas to flow. This is chosen to be the maximum between the cooling time and the free-fall time $t_\mathrm{ff} = (4\pi G\rho_\mathrm{g})^{-1/2}$.

Over the past few years, starting from this general background a number of refinements have been introduced. These mainly concern the criteria to decide whether a gas particle is suitable to form stars, and the way stars emerge from gas, i.e. how gas clouds undergo fragmentation.

Navarro & White (1993) and Katz, Weinberg & Hernquist (1996) introduce an additional condition for the onset of SF, i.e. the so-called overdensity criterion, which assures that a collapsing cloud remains cool. The threshold density implies that the cooling time-scale is much shorter than the dynamical time-scale, and this always occurs for temperatures greater than the cut-off temperature of the cooling curve ($T = 10^4$ K for the typical mass resolution of this type of problem). In addition to this, Katz et al.

(1996) impose the condition that the gas particles can form stars only if a minimum physical density corresponding to 0.1 hydrogen atoms per cm^3 is met.

In Katz et al. (1996) and Navarro & White (1993), the fragmentation of a gas cloud is usually modelled in the following way. When in a gas particle SF switches on, the gaseous mass decreases until it reaches some minimum value, say 5 per cent of the original value. At this stage, the gas particle is turned into a collisionless star particle, while the remaining gas is distributed among the surrounding gas particles. In the meantime the gas particle is considered as a dual entity, whose mass is partly collisionless and partly collisional. This approach is a good compromise in terms of computational effort because it is not necessary to add a collisionless particle every time a new star is formed (Katz et al. 1996). Then the choice of the star-forming regions is made by means of suitable probability arguments. Every time a gas particle forms stars, its mass is reduced by one-third (free parameter). A different value is adopted by Navarro & White (1993), who suppose that at each star-forming event the gas mass is halved, and that each gas particle can split into four star particles at most (this limit is set by computational limitations).

A somewhat different scheme is followed by Steinmetz (1996), who calculates the mass of the newly born star particle using equation (1) in the form:

$$m_\star = m_g\left[1 - \exp\left(-\frac{c_\star \Delta t}{t_{ff}}\right)\right], \qquad (2)$$

where Δt is the particle time-step. The mass of the gas particle is accordingly reduced. Although this latter approach appears to be more physically sound, computational problems can arise when many star particles are expected to form, so that the number of star formation episodes must be artificially limited.

Once stars are present, they are expected to return to the interstellar medium (ISM) part of their mass (in the form of chemically processed gas) and energy via supernovae (SNe) explosions, stellar winds and ultraviolet (UV) flux. These latter contributions are significant only in the case of massive stars. All this is known as the stellar energy feedback (FB).

The amounts of mass, metals and energy released by each star depend on a star's mass, lifetime and initial composition in a way that can be easily taken into account.

The key problem here is to know how the energy released by stars is given to the ISM because the limited resolution of N-body simulations does not allow one to describe the ISM as a multiphase medium. Basically two different schemes exist:

(i) All the energy (from SNe, stellar winds and UV flux) is given to the thermal budget of the fluid element (Katz 1992; Steinmetz & Müller 1994).

(ii) Only a fraction of this energy is allowed kinetically to affect the surrounding fluid elements. This fraction (f_v or ϵ_{kin}) is a free parameter (Navarro & White 1993; Mihos & Hernquist 1994) chosen in such a way that some macroscopic properties of the galaxy, like for instance the metallicity distribution (Groom 1997) or the shape of the disc (Mihos & Hernquist 1994), are reproduced.

The depositing of all the energy in the thermal budget of the fluid (first alternative) has little effect on the structure and evolution of a galaxy. In fact, since the thermal energy is given to a medium of high density and short cooling time-scale in turn, it is almost immediately radiated away. The difficulty cannot be cured by supposing that the thermal energy is injected and shared over an e-folding time-scale (Summers 1993).

In all the above schemes the fraction of energy from stellar FB that is not transformed into kinetic energy is added to the energy budget of the fluid element, and the fluid element is allowed to cool. The integration of the energy equation with respect to time is generally made according to a semi-implicit scheme (see the discussion in Hernquist & Katz 1989).

In this paper we present in detail our prescriptions for computing energy balance, SF and FB. The organization of the paper is as follows. Section 2 describes the numerical code and the method used to integrate the energy equation, whereas Section 3 discusses in detail the adopted initial conditions. In Section 4 we test our energy integration scheme following the formation of a galactic disc. Section 5 presents a discussion on various SF criteria, our new approach to SF and the corresponding models. Section 6 examines the effects of different sources of FB, while some concluding remarks are presented in Section 7.

2 THE BASIC NUMERICAL TOOL

2.1 The tree–SPH code

All the simulations presented here have been performed using the tree–SPH (smoothed particle hydrodynamics) code developed by Carraro (1996) and Lia (1996), and described by Carraro, Lia & Chiosi (1998a), to whom the reader is referred for all details.

The code, which can follow the evolution of a mix of dark matter (DM) and baryons (gas and stars), has been carefully checked against several classical tests with satisfactory results, as reported in Carraro et al. (1998a).

In this code, the properties of the gas component are followed by means of the smoothed particle hydrodynamics (SPH) technique (Lucy 1977; Gingold & Monaghan 1977;Benz 1990), whereas the gravitational forces are computed by means of the hierarchical tree algorithm of Barnes & Hut (1986) using a typical tolerance parameter $\theta = 0.8$ and expanding tree nodes to quadrupole order. We adopt a Plummer softening parameter.

In SPH each particle represents a fluid element whose position, velocity, energy, density, etc. are followed in time and space. The properties of the fluid are locally estimated by an interpolation that involves the smoothing length h_i. In our code each particle possesses its own time and space variable smoothing length h_i, and evolves with its own time-step. This renders the code highly adaptive and flexible, and suited to speed up the numerical calculations.

Radiative cooling is described by means of numerical tabulations as a function of temperature and metallicity taken from Sutherland & Dopita (1993). This allows us to account for the effects of variations in the metallicity among the fluid elements and for each of these as a function of time and position.

The chemical enrichment of the gas particles caused by SF and stellar ejecta (Portinari, Bressan & Chiosi 1998) is described by means of the closed-box model applied to each gas particle – cf. Carraro et al. (1998a) and Carraro, Lia & Buonomo (1998b) for more details. Star formation and feedback are discussed below.

All the calculations presented here have been carried out on a Digital Alpha-2000 (330 MHz, 512 Mbyte RAM) workstation hosted by the Padua Observatory & Astronomy Department.

2.2 On the integration of the energy equation

The usual form of the energy equation in SPH formalism is

$$\frac{\mathrm{d}u_i}{\mathrm{d}t} = \sum_{j=1}^{N} m_j \left(\frac{\sqrt{P_i P_j}}{\rho_i \rho_j} + \frac{1}{2}\Pi_{ij} \right) \boldsymbol{v}_{ij} \times \frac{1}{2}[\nabla_i W(r_{ij}, h_i) + \nabla_i W(r_{ij}, h_j)] + \frac{\Gamma - \Lambda_{\mathrm{C}}}{\rho}, \quad (3)$$

(Hernquist & Katz 1989; Benz 1990). The first term represents the heating or cooling rate of mechanical nature, whereas the second term Γ is the total heating rate from all sources apart from the mechanical ones, and the third term $\Lambda_{\mathrm{C}}/\rho$ is the total cooling rate by many physical agents (see Carraro et al. 1998a for details).

In the absence of explicit sources or sinks of energy, the energy equation is adequately integrated using an explicit scheme and the Courant condition for time-stepping (Hernquist & Katz 1989).

The situation is much more complicated when considering cooling. In fact, in real situations the cooling time-scale becomes much shorter than any other relevant time-scale (Katz & Gunn 1991), and the time-step becomes considerably shorter than the Courant time-step, even using the fastest computers at our disposal. This fact makes it impossible to integrate the complete system of equations (cf. Carraro et al. 1998a) adopting as time-step the cooling time-scale.

To cope with this difficulty, Katz & Gunn (1991) damp the cooling rate to avoid too short time-steps, allowing gas particles to lose only half of their thermal energy per time-step.

Hernquist & Katz (1989) and Davé, Dubinski & Hernquist (1997) solve equation (3) semi-implicitly using the trapezoidal rule,

$$u_i^{n+1} = u_i^n + \tfrac{1}{2}(\mathrm{d}t_i^n \times e_i^n + \mathrm{d}t_i^{n+1} \times e_i^{n+1}), \quad (4)$$

where $e_i = \mathrm{d}u_i/\mathrm{d}t$. The leap-frog scheme is used to update the thermal energy, and the energy equation, which is non-linear for u_j, is solved iteratively both at the predictor and at the corrector phase. The technique adopted is a hybrid scheme that is a combination of the bi-section and Newton–Raphson methods (Press et al. 1989). The only assumption is that at the predictor stage, when the predicted $\tilde{u}_i^{n+1}$ is searched for, the terms u_i^{n+1} are equal to u_i^{n-1}.

Our scheme to update the energy is conceptually the same, but differs in the predictor stage and in the iteration scheme adopted to solve equation (4). In brief, at the first time-step the quantity $u^{n-1/2}$ is calculated, and for all subsequent time-steps the leap-frog technique, as in Steinmetz & Müller (1993), is used:

(i) Start with u^n at t^n.
(ii) Compute $\tilde{u}^n$ as

$$\tilde{u}^n = u^{n-1/2} + \tfrac{1}{2} t^n \times e^n.$$

This predicted energy, together with the predicted velocity, is used to evaluate the viscous and adiabatic contributions to e_i^{n+1}. In other words the predictor phase is calculated explicitly because all the necessary quantities are available from the previous time-step t^n.

(iii) Derive u^{n+1} by solving equation (4) iteratively (corrector phase) for both the predicted and old adiabatic and viscous terms.

In the corrector stage the integration of equation (4) is performed using the Brent method (Press et al. 1989) instead of the Newton–Raphson, the accuracy being fixed to one part in 10^{-5}. The Brent method has been adopted because it is better suited as a root-finder for functions in tabular form (Press et al. 1989).

3 INITIAL CONDITIONS

In the following we are going to check our treatment of the energy equation and our implementation of SF and FB by simulating the formation of a disc galaxy. Since our code is not a cosmological code we shall consider an ad hoc initial configuration for a protogalaxy. This approach is justified by the fact that we are going to focus on processes occurring at scales much smaller than the cosmological ones.

3.1 Theoretical overview

According to modern gravitational instability theory (White & Rees 1978), protogalaxies comprise a mixture of dissipationless dark matter (DM), whose nature is so far not clear, and dissipational baryonic material, roughly in the mass ratio 1:10. After a violent relaxation process, which follows the separation from the Hubble expansion, a DM halo becomes isothermal, and acquires baryonic material which heats up at the halo virial temperature. Gas then cools and collapses, and through fragmentation turns into the stars we see today in discs and spheroidal systems.

In this scenario discs form as a consequence of the angular momentum that DM haloes acquire as a result of the tidal torque felt by surrounding haloes, while spheroidal systems are thought to be produced by merging of discs.

Instead of selecting haloes from cosmological *N*-body simulations (see for instance Weil, Eke & Efstathiou 1998), in our code we set up a protogalaxy as an isolated rotating DM halo with baryonic material inside, proceeding as follows.

3.2 Initial configuration

We consider a triaxial DM halo whose density profile is

$$\rho(r) \propto \frac{1}{r}. \quad (5)$$

Although rather arbitrary, this choice seems to be quite reasonable. Indeed DM haloes emerging from cosmological *N*-body simulations are not King or isothermal spheres, but show – independently of cosmological models, initial fluctuation spectra and total mass – a *universal* profile (Navarro, Frenk & White 1996; Huss, Jain & Steinmetz 1998). This profile is not a power law, but has a slope $\alpha = \mathrm{d}\ln\rho/\mathrm{d}\ln r$ with $\alpha = -1$ close to the halo centre, and $\alpha = -3$ at larger radii. Thus in the inner part the adopted profile matches the *universal* one. Moreover this profile describes a situation that is reminiscent of a collapse within an expanding universe, the local free-fall time being a function of the radius (see the discussion in Aguilar & Merritt 1990; Curir, Diaferio & De Felice 1993). Moreover, triaxiality is quite natural for galactic DM haloes (Becquaert & Combes 1997; Olling & Merrifield 1998).

DM particles are distributed by means of an *acceptance–rejection* criterion, following step by step the procedure developed by Curir et al. (1993). Specifically, we consider a triaxial ellipsoid whose radial scale r is given by

$$r = \left(x^2 + \frac{y^2}{(b/a)^2} + \frac{z^2}{(c/a)^2} \right) \quad (6)$$

where $a > b > c$ are the axial ratios (see Table 1).

The velocity field has been chosen to produce an angular momentum that depends linearly on the distance, $j(r) \propto r$ (Barnes & Efstathiou 1987) (Fig. 1). It has been built up by sampling the

Table 1. Initial conditions of the simulated dark matter halo: $N = 10\,000$; $a : b : c = 3.0 : 2.25 : 1.5$.

λ	β	δ_1	δ_2
0.09	0.20	0.05	0.025

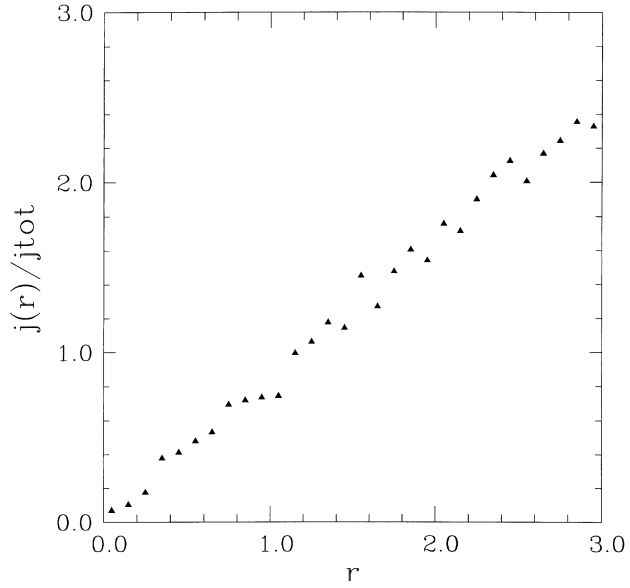

Figure 1. The initial specific angular momentum j as a function of the radial distance r from the centre of a $1/r$ dark matter halo.

moduli V of the particle velocities by using a Maxwellian distribution and imposing that the virial ratio $\beta = 2 \times T/|W|$ is equal to some fixed value ranging between 0.05 and 0.20. Here T is the kinetic energy, while W is the potential energy. The final Cartesian components of particle velocity can be derived from the following formulae:

$$V_x = -V \times \sin(\theta + \alpha) \tag{7}$$

$$V_y = V \times \cos(\theta + \alpha) \tag{8}$$

$$V_z = \xi \tag{9}$$

where θ is the angle between the position vector of a particle and the x coordinate axis, α is an angle varying between $-\delta_1\pi$ and $+\delta_1\pi$, whereas ξ is a random parameter ranging from $-\delta_2 V$ to $+\delta_2 V$; δ_1 and δ_2 are chosen so that the kinetic energy T changes by less than 1 per cent of the value giving the initial virial ratio β.

Table 1 summarizes the adopted initial values for the set of parameters introduced above. Because of the assigned velocity field, the halo acquires an amount of angular momentum, which is conventionally described by means of the dimensionless spin parameter λ:

$$\lambda = \frac{J|E|^{1/2}}{GM^{5/2}}.$$

Here G is the gravitational constant, J the system angular momentum, M the total mass and E the total system energy. In our case the λ parameter has been chosen to be 0.09, significantly greater than the mean values of cosmological haloes (Steinmetz & Bartelmann 1995). This choice is motivated by the comparison we are going to make with similar initial conditions (Navarro & White 1993; Raiteri, Villata & Navarro 1996; Thacker et al. 1999).

The softening parameter ϵ is computed as follows. After plotting the interparticle separation as a function of the distance to the model centre, we compute ϵ as the mean interparticle separation at the centre of the sphere, taking care to have at least one hundred particles inside the softening radius (Romeo & Pearce, private communication). We consider a Plummer softening parameter, equal for both DM and gas particles (see below), and keep it constant along the simulation. For this particular choice of the initial configuration, the softening parameter ϵ turns out to be 3.6 kpc.

Total energy and angular momentum are conserved within 1 per cent and 0.1 per cent levels, respectively. We consider a dark matter halo with mass $10^{12}\mathrm{M}_\odot$ and radius $a = 120$ kpc in order to simulate a galaxy with a size similar to the Milky Way. Axial ratios are $a = 3.00$, $b = 2.25$ and $c = 1.50$.

4 THE FORMATION OF A GASEOUS DISC

The formation of a galactic disc is simulated by distributing gas inside the halo described above and switching on the cooling. To mimic the infall of gas inside the potential well of the halo, we distribute gas particles (10 000 in number) on the top of DM particles. The baryonic fraction adopted is $f_\mathrm{b} = 0.1$, and gas particles are Plummer-softened in the same way as the DM particles.

Under cooling and the velocity field of the halo, the gas is expected to settle down in a rotating thin structure. For this purpose for the baryonic component we need to specify a temperature and a metal content. We assume that the gas has temperature $\approx 1.0 \times 10^4$K (Navarro & White 1993), and an almost primordial metal content amounting to $Z \approx 10^{-4}$, which translates into [Fe/H] ≈ -3 (Bertelli et al. 1994).

This simulation is meant to verify that our energy integration scheme works properly when cooling is switched on. For this reason SF, FB and chemical enrichment are turned off.

The formation of the disc is shown in Fig. 2. The panels follow the evolution of the gas component in the x–z plane. Time is in Gyr. Starting from an ellipsoidal initial configuration ($t = 0.0$), as a result of their cooling and angular momentum baryons settle down in a thin rotating structure ($t = 1.75$), eventually developing a bulge-like structure in the model centre ($t = 2.0$). At this time the gaseous disc is about 5 kpc high and 40 kpc wide. Comparing our results with a similar simulation by Raiteri et al. (1996) we see that in our case the disc forms more slowly. This is because of the lower efficiency of our cooling with respect to the more widely adopted Katz & Gunn (1991) cooling.

5 STAR FORMATION

As already recalled, SF in N-body simulations is allowed to occur if suitable criteria meant to simulate the real behaviour of the ISM are satisfied.

Current prescriptions for SF stand on three time-scales, i.e. the crossing, cooling and free-fall time-scales, which ultimately depend (although in a different fashion) on the density of the fluid. According to the most popular prescription (Katz 1992; Navarro & White 1993), SF can occur if

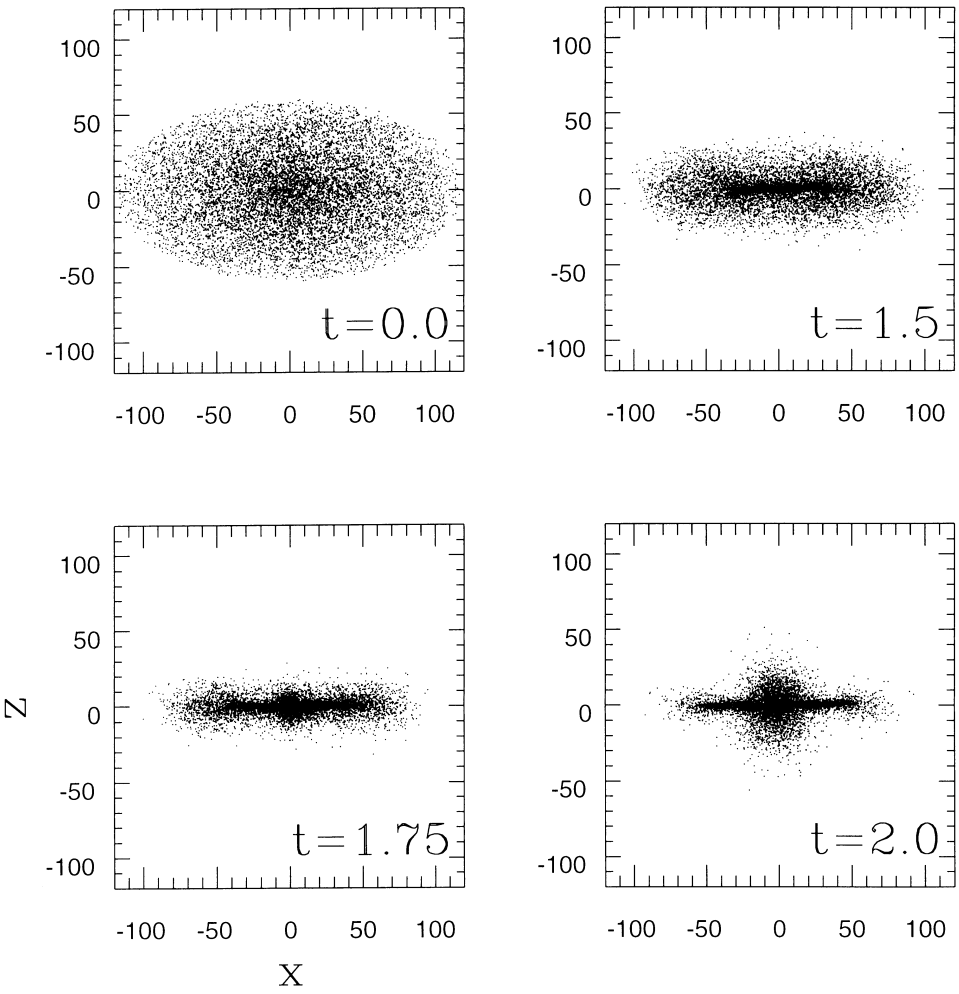

Figure 2. The formation process of a galactic disc in the x–z plane. In the bottom right corner of each panel is reported time in billion years.

(i) $\nabla \cdot \boldsymbol{v}_i < 0$,
(ii) $t_{\rm sound} > t_{\rm ff}$,
(iii) $t_{\rm cooling} \ll t_{\rm ff}$.

The aim of this section is to scrutinize closely the effects of these three conditions on the model results. We start with some general considerations.

Most likely, the divergence criterion is not strictly required. First the typical mass resolution (10^6–10^7 $M_\odot$) of this kind of N-body simulation is clearly not sufficient to follow the kinematical behaviour of the gas at the molecular clouds scale. Then in principle a fluid element can form stars without being in a convergent flow (think about shock-induced or stochastic SF). For instance in the special case of an already formed spiral galaxy Mihos & Hernquist (1994) adopt a different dynamical criterion, based upon the Toomre instability criterion.

The free-fall time-scale is usually computed as

$$t_{\rm ff} = (4\pi G\rho)^{-1/2} \tag{10}$$

where ρ is the gas density of the fluid element. We have replaced this condition with the more general one

$$t_{\rm ff} = (4\pi G\rho_{\rm tot})^{-1/2} \tag{11}$$

where $\rho_{\rm tot} = \rho_{\rm gas} + \rho_{\rm DM}$. In principle, one should consider also $\rho_{\rm star}$. In fact the dynamical behaviour of the fluid element under consideration depends on all the mass inside the volume with radius $2 \times h$, where h is the smoothing length. Therefore at the typical resolution of these simulations (about 2.5 kpc), the presence of DM accelerates the collapse of a fluid element by lowering the free-fall time-scale. DM density is evaluated in the same manner as gas density, defining a smoothing length for any DM particle, although this scheme is computationally expensive. The importance of DM on SF has recently been studied from an analytical point of view by Caimmi & Secco (1997).

Finally, we remind the reader that the condition on the cooling time-scale is customarily replaced by a condition on the density, i.e. a constant density threshold (Navarro & White 1993). This stems from suitable arguments about the cooling time-scale based on the notion that the gas metallicity has no effect. However, as the cooling rate does increase with the metal content of the ISM with consequent increase of the threshold density, the more general condition on the cooling time-scale ought to be preferred.

5.1 Testing the SF recipes

To this end we perform the same simulation as in Section 4, namely formation of a disc galaxy, but letting stars form according to a different set of criteria. We follow the model till the end to the major star formation episode. The simulations have been carried out using 10 000 DM and 10 000 baryonic particles, neglecting in

Table 2. The four test cases.

Case A	$\nabla \cdot \boldsymbol{v}_i < \mathbf{0}$	$t_{\rm sound} > t_{\rm ff}$	$\rho > \rho_{\rm crit}$
Case B		$t_{\rm sound} > t_{\rm ff}$	$\rho > \rho_{\rm crit}$
Case C	$\nabla \cdot \boldsymbol{v}_i < \mathbf{0}$	$t_{\rm sound} > t_{\rm ff}$	$t_{\rm cooling} \lll t_{\rm ff}$
Case D		$t_{\rm sound} > t_{\rm ff}$	$t_{\rm cooling} \lll t_{\rm ff}$

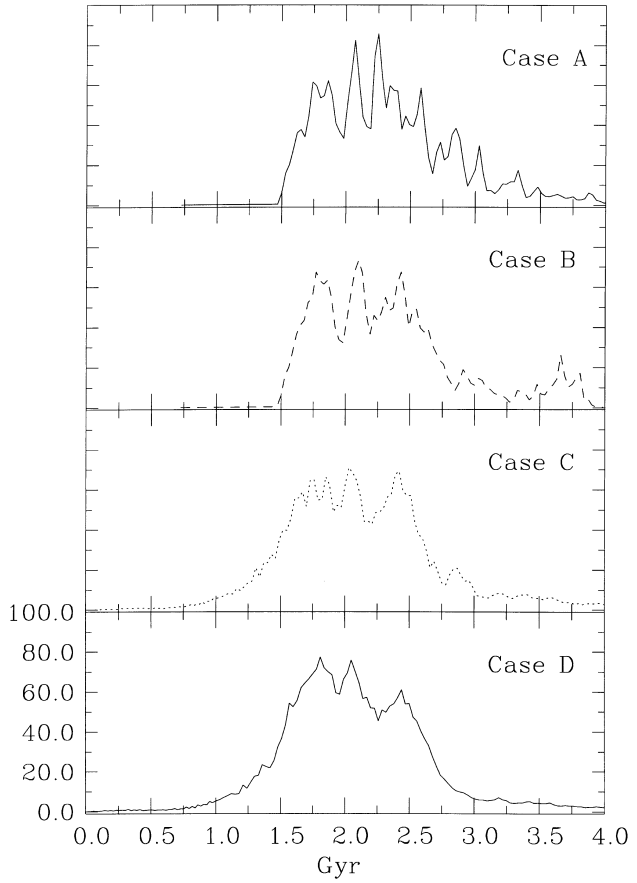

Figure 3. The star formation history (in solar masses per year) for four models in which star formation criteria are defined as in Section 5. See text for details.

Table 3. Comparison of SF criteria.

Case	SF peak ($\mathrm{M_\odot\ yr^{-1}}$)	Peak time (Gyr)	Stars formed (number)
A	85	2.25	3381
B	73	2.10	3771
C	71	2.03	6580
D	77	1.81	8543

this particular set of models any source of FB. The four cases outlined in Table 2 are examined.

In our models, fragmentation of gas particles undergoing SF is allowed to occur and new star particles are created when the gas content of the fluid element has fallen below 20 per cent of the initial value, the remaining gas being spread out over the surrounding particles. This limits the number of star particles produced. Moreover, a gas particle is allowed to experience up to ten SF episodes. Afterwards it can no longer make stars. In all simulations the efficiency parameter $c_{\rm star}$ is fixed to 0.1. Finally, when more than two star particles form inside a sphere with radius equal to the softening parameter $\epsilon = 3.6$ kpc, they are merged together to form a single object, in order to keep the total number of particles small.

The results for the SFR as a function of time are shown in Fig. 3, whereas a few relevant quantities of the models are given in Table 3. Comparing either case A to case B or case C to case D, we notice that the criterion on the velocity divergence has no effect in practice, as argued above. In contrast, there is a significant difference on passing from the cases A and B based on the overdensity condition to the cases C and D based on the cooling time-scale. In fact the models of the first group start to form stars noticeably later, and after the burst, which occurs somewhat later, SF is higher than in the second group of models, and shows some secondary peaks. Dropping the divergence criterion significantly increases the number of spawned stars (models C and D).

In these models, after the peak, SF proceeds at a rate of around 4–6 $\mathrm{M_\odot\ yr^{-1}}$, quite usual for disc galaxies. Putting together all these differences and the discussion above, we are led to prefer the combination of criteria of model D, which we shall use in all the other simulations presented in this paper. All simulations exhibit the SF peak at about 2 Gyr, much later than, for instance, the Raiteri et al. (1996) simulation. This is clearly the result of the different cooling functions adopted. The analytical formulae of Katz & Gunn (1991) provide a much more efficient cooling (see below and Carraro et al. 1998a).

6 STELLAR FEEDBACK

In this section, we test separately the effect of FB of different nature making use of case D for the recipe of star formation. Furthermore, we include the effect of chemical enrichment.

The energy FB originates from SNe explosions of both types Ia and II (Greggio & Renzini 1983), the stellar winds from massive stars (Chiosi & Maeder 1986) and the UV flux from the same objects (Chiosi et al. 1998).

In order to evaluate the amount of energy injected into the ISM by the above sources, we suppose that each newly formed star particle, which for the mass resolution of our simulations has a total mass of the order of 10^7 $\mathrm{M_\odot}$, is actually made up of a larger number of smaller subunits (the real stars) lumped together and distributed in mass according to a given initial mass function (IMF). For the purposes of the present study we adopt the IMF given by Miller & Scalo (1979) over the mass interval from 0.1 to 120 $\mathrm{M_\odot}$.

Chemical evolution is followed by means of the closed-box approximation (Tinsley 1980; Portinari et al. 1998) and sharing of the metals among the gas particles is described by means of a diffusive scheme (Groom 1997; Carraro et al. 1998a).

Details on implementation of FB in our tree–SPH code have already been reported in Carraro et al. (1998a), to which the reader should refer. With respect to the previous study, only two major changes have been made. First, of the UV flux emitted by massive stars, only a small fraction (0.01) is actually used. All the remaining UV flux is supposed to be reprocessed by dust into the far-infrared and lost by the galaxy (Silva et al. 1998). Secondly, the energy released to the ISM by a SN event amounts only to 10^{50} erg, roughly 10 times less than in older evaluations – see Thornton et al. (1998) for an exhaustive discussion of this topic. The heating rates from the three sources of energy are displayed in Fig. 4 for

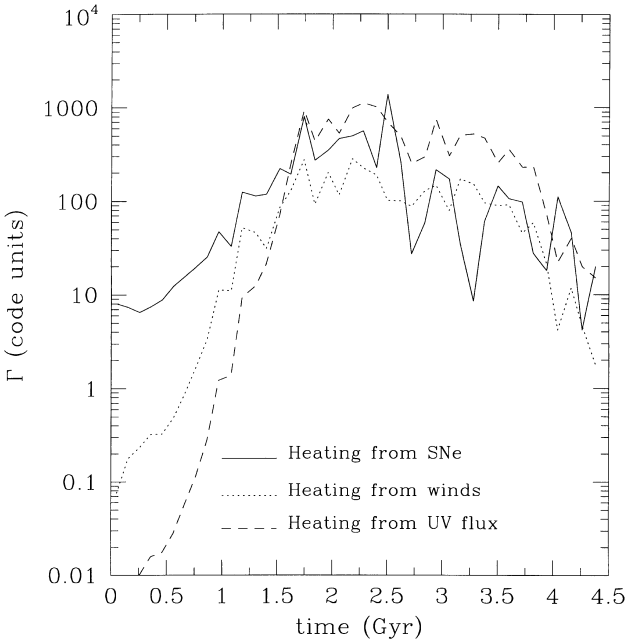

Figure 4. The heating rates from the three sources of FB as indicated. See text for more details.

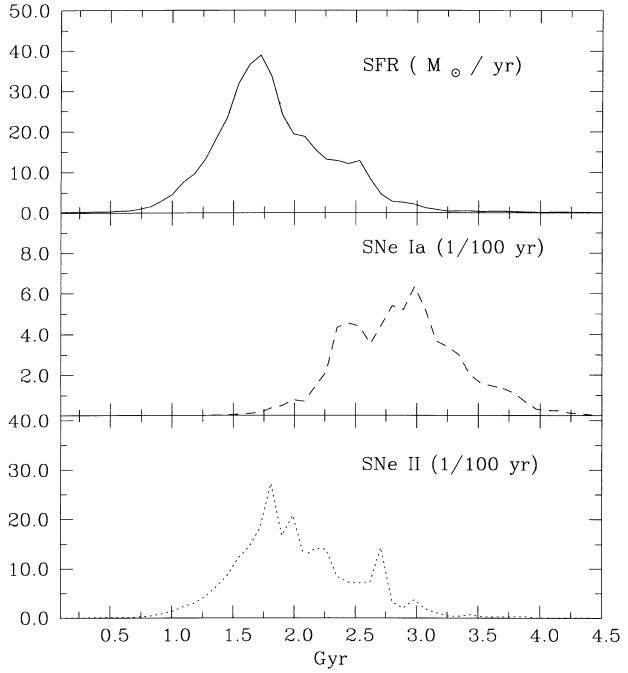

Figure 5. Star formation history and SNe rates for the model D3. SNe II closely follow SF history, whereas SNe Ia exhibit a peak somewhat later, as expected from the different lifetime of their progenitors.

the sake of illustration. A notable feature to remark upon is that the energy injection by stellar winds may parallel that from SNe explosions, and the contribution from the UV flux plays a significant role although a strong dumping factor has been applied. All the FB mechanisms have almost the same trend, since they derive basically from the same stellar sources.

Finally, we stress that all the energy from FB is given to the thermal budget of the particles, because at the resolution with which we are working it is impossible to describe this process in more detail. In fact, the space resolution of these simulations is about 2.5 kpc, much larger than the typical distance over which the effects of SNe explosions and stellar winds are visible (McKee & Ostriker 1977) – see also the arguments given by Carraro et al. (1998a). Possible interactions of kinetic nature among gas particles occur only via the pressure gradients.

6.1 Testing the sources of feedback

In order to understand the role played by each source of FB, we perform the following experiments using the same model as in the previous section. Three cases are considered:

(i) Case D1: FB from SNe;
(ii) Case D2: FB from SNe and stellar winds;
(iii) Case D3: FB from SNe, stellar winds and UV flux.

First of all, for the case D1, consider the SF history, and the rate of SNe of both types, Ia and II. Owing to the different stellar progenitors, the rates of SNe Ia and II show different trends. SNe II explode immediately, and their rates strictly follow the SF history. On the contrary, SNe Ia start to appear later, the progenitor being less massive. The relative abundance of SNe events clearly depends on the adopted IMF. In Fig. 5, we illustrate the SF history and the SNe rates for case D3.

The results of these three simulations are shown in the various panels of Fig. 6. A few relevant quantities of the models are given in Table 4. Namely we consider the mean gas temperature, the SF peak and the time at which it occurs, the final maximum metal abundance, and the radial and vertical dimensions of the final stellar disc.

Looking at these results the following conclusions can be drawn. The models D1 and D2 do not differ significantly: by simply turning on FB from stellar winds, the final models becomes a bit hotter, fewer stars are formed and the final maximum metal abundance achieved is slightly lower. Since almost the same amount of stars are generated, the final stellar disc morphology is basically identical.

When the combined effects of all the FB sources are considered (model D3), the situation changes more significantly (see also Fig. 4). The model becomes hotter more rapidly when SF starts, the SF peak occurs earlier, and fewer stars are formed. As a consequence the final mean temperature is somewhat lower and the disc morphology is not as well resolved as in the previous models. The final maximum metallicity turns out to be somewhat greater owing to the effect of diffusive mixing. Metals are spread out evenly around the gas neighbours. Since SF in this model stops early, no metal-poor stars are produced, and the mean metallicity increases.

In all the models a number of gas particles do not experience SF and keep the primordial metal content.

7 SUMMARY AND CONCLUSIONS

In the framework of the formation of a spiral-like galaxy, we have examined in detail the effect of different prescriptions for star formation and feedback on numerical simulations of galaxy formation and evolution.

First of all we described in detail how we integrate the energy equation when cooling is switched on. We adopted cooling

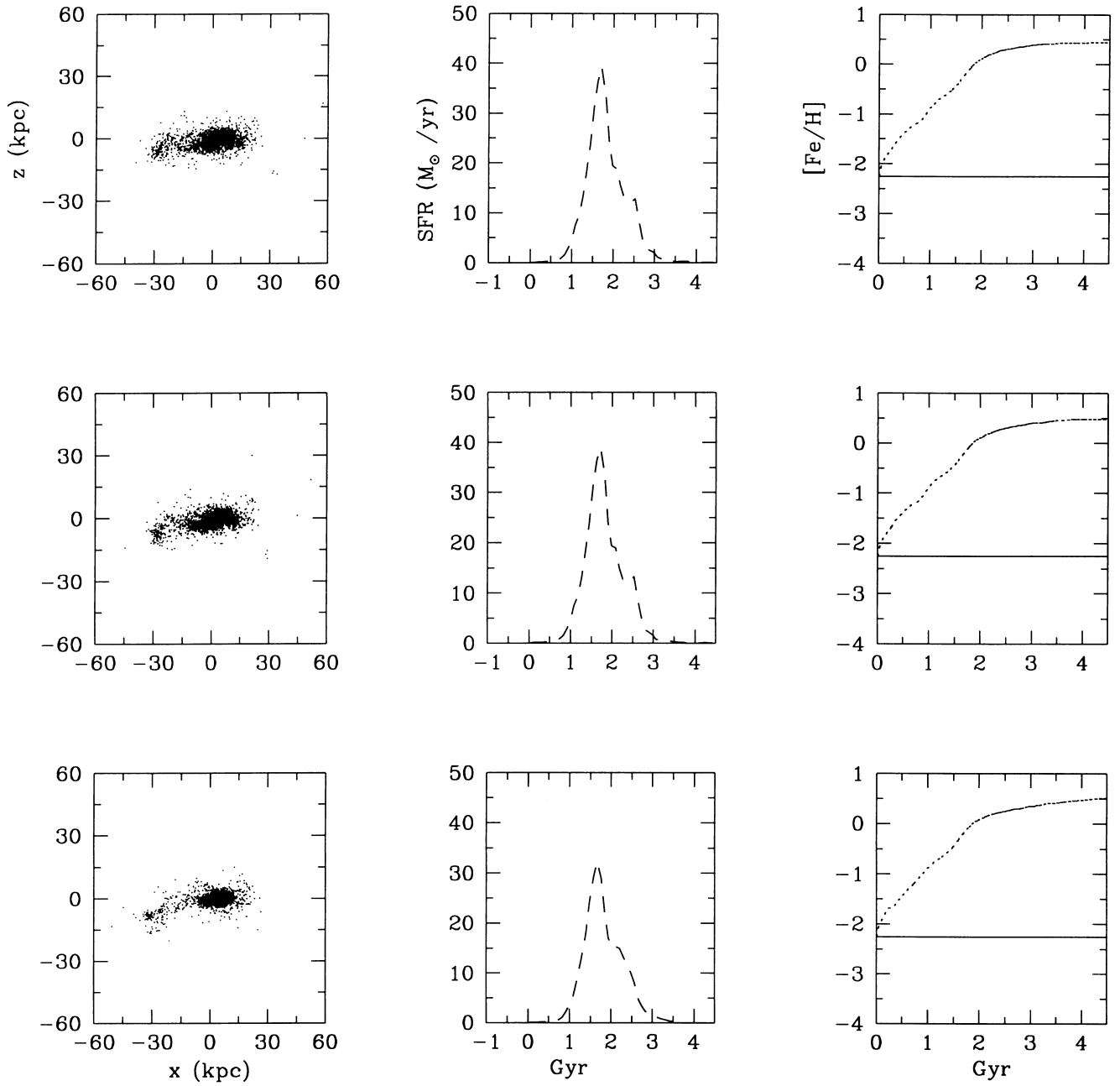

Figure 6. Comparison of the evolution of the galactic models by using different sources of feedback. The top row shows the evolution of a model (D1) in which only SNe FB is considered, the middle row a model (D2) in which also stellar winds are switched on, and the bottom row the case of a model (D3) in which all the FB sources are allowed to act. Right-hand panels show the chemical enrichment (solid line, the maximum metallicity; dotted line, the minimum), middle panels the SF history, and left-hand panels the final morphology of the stellar disc.

Table 4. Results for models with different feedback.

Case	T_{ave} (10^6 K)	SF peak ($M_\odot$ yr^{-1})	Peak time (Gyr)	$[Fe/H]_{fin}$ (dex)	r_D (kpc)	h_D (kpc)
D1	1.15	39	1.72	0.446	30	5
D2	1.46	38	1.72	0.406	30	5
D3	1.33	32	1.67	0.513	20	5

functions that depend on metal abundance, and use the Brent method as root-finder instead of the more widely used Newton–Raphson scheme. The Brent scheme performs better when using functions in tabular form.

Concerning the physical conditions at which star formation is likely to start, we argue that the criterion on the velocity divergence has no sizeable effect on the model results. Moreover the overdensity and cooling time criteria are equivalent only if the effect of metallicity on the cooling time-scale is neglected. However, because in real galaxies the metallicity varies as a function of time and space, the criterion based on the cooling time-scale ought to be preferred. This finding is a step further towards a better understanding of the conditions under which star formation takes place in real galaxies. In addition in the gas free-fall time computation we introduce the contribution of DM and eventually stars that lie within the neighbouring sphere. This has

the effect of decreasing the free-fall time, thus accelerating the cloud collapse.

Finally we have quantitatively shown the separate and cumulative effects of different sources of feedback (SNe, stellar wind and UV flux from massive stars) on the global properties (SFR, metallicity and morphology) of galaxy models.

ACKNOWLEDGMENTS

The authors gratefully acknowledge an anonymous referee for the detailed report on the first version of this paper. This study has been financed by several agencies: the Italian Ministry of University, Scientific Research and Technology (MURST), the Italian Space Agency (ASI), and the European Community (TMR grant ERBFMRX-CT-96-0086).

REFERENCES

Aguilar L. A., Merritt D., 1990, ApJ, 354, 33
Barnes J. E., Efstathiou G., 1987, ApJ, 319, 575
Barnes J. E., Hut P., 1986, Nat, 324, 446
Becquaert J. F., Combes F., 1997, A&A, 325, 41
Benz W., 1990, in Buchler J. R., ed., Numerical Modelling of Nonlinear Stellar Pulsation. Kluwer, Dordrecht, p. 269
Bertelli G., Bressan A., Chiosi C., Fagotto F., Nasi E., 1994, A&A, 106, 275
Caimmi R., Secco L., 1997, in Persic M., Salucci P., eds, ASP Conf. Ser. Vol. 117, Dark and Visible Matter in Galaxies. Astron. Soc. Pac., San Francisco, p. 456
Carraro G., 1996, PhD thesis, Padova Univ.
Carraro G., Lia C., Chiosi C., 1998a, MNRAS, 297, 1021
Carraro G., Lia C., Buonomo F., Salucci P., 1998b, DM – Italia 1997. Studio Editoriale, Fiorentino, p. 169
Chiosi C., Maeder A., 1986, ARA&A, 24, 329
Chiosi C., Bressan A., Portinari L., Tantalo R., 1998, A&A, 339, 355
Curir A., Diaferio A., De Felice F., 1993, ApJ, 413, 70
Davé R., Dubinski J., Hernquist L., 1997, New Astron., 2, 3, 277
Frenk C. C., Baugh C. M., Cole S., Lacey C., 1997, in Persic M., Salucci P., eds, ASP Conf. Ser. Vol. 117, Dark and Visible Matter in Galaxies. Astron. Soc. Pac., San Francisco, p. 335
Gerritsen J., 1997, PhD thesis, Groningen Univ.
Gingold R. A., Monaghan J. J., 1977, MNRAS, 181, 375
Greggio L., Renzini A., 1983, A&A, 118, 217
Groom W., 1997, PhD thesis, Cambridge Univ.
Hernquist L., Katz N., 1989, ApJS, 70, 419
Huss A., Jain B., Steinmetz M., 1998, ApJ, 517, 64
Katz N., Gunn J. E., 1991, ApJ, 377, 365
Katz N., 1992, ApJ, 391, 502
Katz N., Weinberg D. H., Hernquist L., 1996, ApJS, 105, 19
Lia C., 1996, Master's thesis, Padova Univ.
Lucy L., 1977, AJ, 82, 1013
McKee C. F., Ostriker J. P., 1977, ApJ, 218, 148
Mihos J. C., Hernquist L., 1994, ApJ, 437, 611
Miller G. E., Scalo J. M., 1979, ApJS, 41, 513
Navarro J. F., White S. D. M., 1993, MNRAS, 265, 271
Navarro J. F., Frenk C. S., White S. D. M., 1996, ApJ, 462, 563
Olling R. P., Merrifield M. R., 1998, MNRAS, 297, 943
Portinari L., Bressan A., Chiosi C., 1998, A&A, 334, 505
Press W. H., Flannery B. P., Teukolsky S. A., Vetterling W. T., 1989, Numerical Recipes. Cambridge Univ. Press, Cambridge
Raiteri C. M., Villata M., Navarro J. F., 1996, A&A, 315, 105
Schmidt M., 1959, ApJ, 129, 243
Silva L., Granato G. L., Bressan A., Danese L., 1998, ApJ, 509, 103
Steinmetz M., Bartelmann M., 1995, MNRAS, 272, 570
Steinmetz M., Müller E., 1993, A&A, 268, 391
Steinmetz M., Müller E., 1994, A&A, 281, L97
Steinmetz 1996, in M., Bender R., Davies R. L., eds, New Light on Galaxy Evolution. Kluwer Academic, Dordrecht, p. 259
Summers F. J., 1993, PhD thesis, Univ. California, Berkeley
Sutherland R. S., Dopita M. A., 1993, ApJS, 88, 253
Thacker R. J., Tittley E. R., Pearce F. R., Couchmann H. M. P., Thomas P. A., 1999, MNRAS, in press
Thornton K., Gaudlitz M., Janka H.-Th., Steinmetz M., 1998, ApJ, 500, 95
Tinsley B. M., 1980, Fund. Cosmic Phys., 5, 287
Weil M. L., Eke V. R., Efstathiou G., 1998, MNRAS, 300, 773
White S. D. M., Rees M. J., 1978, MNRAS, 183, 341

This paper has been typeset from a TEX/LATEX file prepared by the author.